

Development of a hillslope model for predicting erosion and water quality impacts of wildfire in SE Australia

¹Sheridan, G., Lane, P. and Noske, P.

¹School of Forest and Ecosystem Science, The University of Melbourne E-Mail: sheridan@unimelb.edu.au

Keywords: water pollution, bushfire, soil erosion, forest.

EXTENDED ABSTRACT

Forest fire is known to lead to increases in sediment and nutrient yield from burnt catchments. A program of hillslope-scale field measurement was initiated following a severe forest wildfire in Victoria in 2003 to quantify the changes in site properties and erosion processes due to the fire. Experimental methods included rainfall simulation, overland flow studies, water repellence testing, concentrated flow erosion measurement, vegetation cover assessment, and ring infiltrometer measurements.

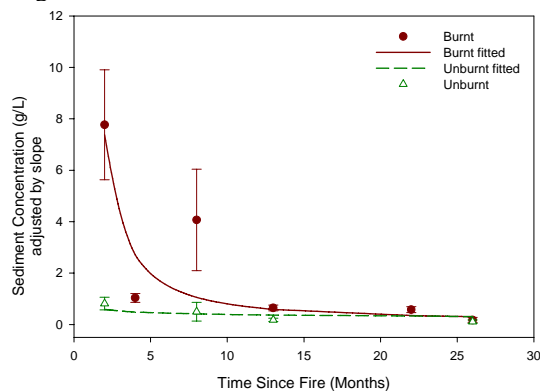


Figure 1. Temporal change in slope-adjusted sediment concentration for burnt and unburnt sites. Error bars are ± 1 standard error.

The results from a series of 100 mm h⁻¹ rainfall simulation experiments over a two year period are shown in Figure 1 and Figure 2, and indicate that;

- there is a large natural seasonal oscillation in water repellence and runoff generation (from rainfall simulation), however burnt and unburnt sites generate similar rates of runoff in summer ie. fire does *not* result in large increases in repellence and runoff in summer
- strong water repellence persists into the wet season at the burnt sites, contributing to greater winter runoff generation (from rainfall simulation)
- the soil infiltration *capacity* (the maximum rate of water intake) remained very high

(400-1300 mm h⁻¹) throughout the study for both burnt and unburnt sites

- the sediment concentration of rainfall-excess overland flow increased approximately 20 fold following the fire and declined exponentially to pre-fire levels two years after the fire

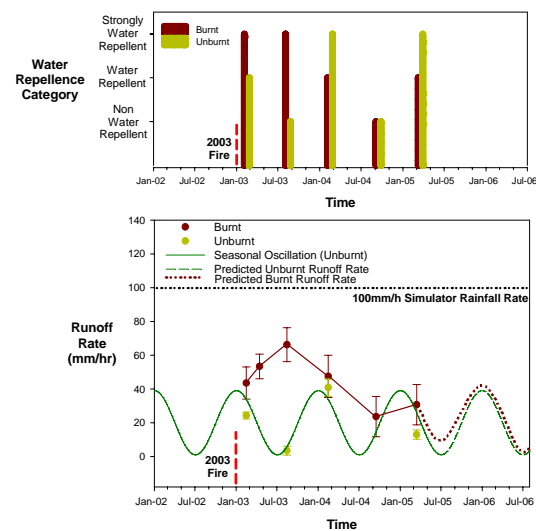


Figure 2. Temporal change in runoff rate (lower graph) and water repellence (upper graph) for burnt and unburnt sites. Error bars are ± 1 standard error.

The results were used to develop a conceptual model of the hillslope processes driving increases in sediment exports following the fire, including; a function to represent runoff generation from areas with *spatially variable* infiltration capacity; a function to represent the seasonal oscillation in water repellence and runoff generation, and post-fire modification to this seasonal pattern, and; a function to represent the change in interill sediment generation rates as a function of time since the fire .

The unexpected conclusion from this study is that the source of elevated post-fire stream sediment loads in *these* catchments is *not* broadscale hillslope erosion. Rather, the very high-spatially variable infiltration capacities result in infiltration excess overland flow and associated erosion from only a small hillslope fringe adjacent to the stream edge.

1. BACKGROUND

Forest fire is known to lead to increases in water, sediment, and nutrient yield from burnt catchments. However measurements from instrumented catchments have shown large variations in the magnitude of these increases (Lane *et al.* 2004; Sheridan *et al.* 2004). Following a severe forest wildfire in Victoria 2003, a program of hillslope-scale field measurements was initiated to quantify the changes in site properties and erosion processes due to the fire. The aim of this research program was to develop a better understanding of the factors affecting rates of erosion and sediment yield following fires.

The two (136 ha and 244 ha) East Kiewa research catchments are located 20 km south of Mt Beauty in the Victorian North East alpine region, part of the Great Dividing Range. The annual rainfall is 1800 mm with some winter snowfall above 1000 m. Mean daily maximum temperature is 17.2° and mean daily minimum is 5.4°. The geology is highly faulted gneiss, quartz diorite and small areas of granodiorite and the topography is steep with elevations ranging from of 600 -1500 m.

Soils are < 1.5 m deep comprised of strongly aggregated clay-loams and sandy clay-loams grading to coarse sand C horizons. Vegetation is open eucalypt forest with the lower areas consisting of mixed species and the upper areas dominated by alpine ash (*E.delegatensis*). Both catchments were burnt in 2003 at sufficient intensity to remove all ground cover, cause the death of the alpine ash, and scorch the crowns of the mixed species Eucalypts.

This paper describes the initial steps in the development of a conceptual model to predict hillslope scale sediment yield from burnt and unburnt forested catchments in SE Australia.

2. EXPERIMENTAL METHODS

To quantify and enable prediction of changes in infiltration excess overland flow and hillslope erosion rates, the following field methods were used at regular intervals for the two year period following the fire;

- water repellence tests using a simplification of the molarity of ethanol droplet test described by King (1981).
- rainfall simulation on three replicates of 1.5 m wide by 2.0 m long plots at 100 mm h⁻¹ for 30

min to measure runoff and interrill sediment generation

- ponded ring infiltrometer measurements (300mm diameter) to quantify the *infiltration capacity* of the soil
- *confined* overland-flow experiments using plots 3.0 m long by 0.15 m wide to measure rill sediment generation rates
- *unconfined* overland-flow studies involving the measurement of application rates and wetted areas to characterize the hydraulic properties of the hillslopes at larger scales
- vegetation survey using transects to estimate cover level

These methods are described in greater detail in Lane *et al.* (2004) and Sheridan *et al.* 2005.

3. RESULTS AND DISCUSSION

3.1. Rainfall simulation

The temporal change in the sediment concentration of runoff following the fire from the rainfall simulation plots is shown in Figure 1. Steady-state sediment concentration values (adjusted for slope) for the rainfall simulation plots at 100 mm h⁻¹ on unburnt plots were in the range 0.11 to 0.81 g L⁻¹. Sediment concentrations from the burnt plots were approximately 20-50 times greater than from the unburnt plots immediately after the fire. However one year later, after an increase in vegetation cover to 50%, the burnt plots produced sediment concentrations that were only 5 times greater than the unburnt plots, and by 26 months the burnt and unburnt sites were producing similar sediment concentrations, at 0.17 and 0.10 g L⁻¹ respectively. The very low sediment concentration recorded in April 2003 is believed to be due to 80 mm of rain in the 4 days prior to the simulation run, which may have reduced available sediment levels for the simulated rainfall events.

It should be noted that the decline in the sediment concentration of runoff shown in Figure 1 may be a function of either temporal change in soil erodibility, or vegetation recovery. The development of expressions to represent these properties as a function of time since the fire is shown in Section 4.3.

The positive relationship between the water repellence class and the runoff generation rate can be seen from inspection of Figure 2. The upper chart illustrating the water repellence category and the lower chart of the runoff rate share a common

horizontal scale allowing the incidence of water repellence to be related to the runoff rate. The seasonal oscillation in water repellence for the *unburnt* soils is evident, with high water repellence recorded in summer/autumn, and low water repellence in winter/spring.

Winter/spring water repellence in the first wet season following the fire was clearly maintained at summer levels for the burnt sites, which may partially account for the increased winter runoff rates recorded at the burnt sites. However the *increase* in runoff over the first winter following the fire suggests there are processes additional to water repellency causing increased runoff at the burnt sites. It is suggested that this increase is due to a washing-in of the ash layer resulting in blocked soil pores, and additional laboratory experiments are underway to test this hypothesis.

The data in Figure 2 also indicate that the runoff generation rates at the burnt sites are returning to the seasonal pattern shown for the unburnt sites. Mathematical expressions that will represent the observed effect of water repellence and fire on runoff generation are presented in Section 4.2.

3.2. Infiltration capacity measurements

The net *infiltration capacity* of heterogeneous and macro-porus forest soils is inherently difficult to quantify. Infiltration capacity in this study was estimated using a range of methods at different scales, including ring infiltrometer, unconfined overland flow experiments, and confined overland flow experiments.

It is important to note that while rainfall simulation provides information on the *infiltration rate*, (I_r) it does not necessarily indicate the net *infiltration capacity* (I_{nc}) of the soil, unless the rainfall rate exceeds the point infiltration capacity (I_{pc}) at *every* point on the plot. Even when runoff is generated under the rainfall simulator, this doesn't mean that I_{nc} has been exceeded. There may be many points on the rainfall simulator plot where the *capacity* for infiltration is not satisfied by the *supply* of runoff water to that particular point.

Results from the ring infiltrometer experiments conducted in September (wet) and March (dry) are summarized in Table 1. The measured *infiltration capacity* is very high for both the burnt and unburnt sites, in the range 400-1300 mm h⁻¹.

Table 1. Mean saturated hydraulic conductivity values measured using the single ring infiltrometer. Standard deviation and number of replicates are given in parenthesis.

Treatment	Soil water status	Infiltration Rate (mm hr ⁻¹)
Burnt	Dry ^B	970 (500, 6)
	Wet ^A	400 (200, 6)
Not burnt	Dry ^B	730 (120, 6)
	Wet ^A	1300 (800, 6)

A: Measured in September

B: Measured in March

The magnitude of these results from the ring infiltrometer experiments are compared to results from unconfined overland flow experiments and from confined overland flow experiments in Table 2. These results support the ring infiltrometer data and indicate that I_{nc} is an order of magnitude higher than the 70 mm h⁻¹. value determined for I_r from the rainfall simulation experiments. The results from all of these measurement methods confirms that I_{pc} is highly variable, resulting in high variability between replicates of I_{nc} measurement (as shown by the large SD value).

Table 2 Comparison of infiltration measurements (I_r and I_{nc}) using a range of experimental methods. All measurements are for burnt, dry, sites in 2005.

Method (and parameter)	Area (m ²)	Mean	SD	n
Rainfall simulator (I_r)	3	70	--	3
Ring infiltrometer (I_{nc})	0.07	1000	500	6
Overland flow (I_{nc})	6-14	1200	500	10
Shear stress exp't (I_{nc})	0.45	1100	700	8

Value for rainfall simulation is the *infiltration rate* not the *infiltration capacity*

The high value of (I_{nc}) suggests that surface runoff would not be generated under simulated 100 mm h⁻¹ rainfall, however the rainfall simulator results show that this is not the case. The implications of this large difference between I_r and I_{nc} are very important with respect to runoff model selection and development, and are explored further in Section 4.2.

3.3. Results and Discussion - Summary

The results show that;

- there is a large natural seasonal oscillation in water repellence and runoff generation (from rainfall simulation) for the forest soils of the East Kiewa.
- burnt and unburnt sites generate similar rates of runoff in summer ie. fire does *not* result in large increases in water repellence and runoff (from rainfall simulation) in summer
- water repellence persists more strongly into the wet season at the burnt sites, contributing to increased winter runoff generation (from rainfall simulation) in the burnt areas
- the soil infiltration *capacity* (the maximum rate of water intake) remained very high (around 1000 mm h⁻¹) throughout the study for both burnt and unburnt sites, indicating that the broadscale generation of overland flow in these catchments is very unlikely, even after high intensity fire
- the sediment concentration of rainfall-excess overland flow increased approximately 20-50 fold following the fire and declined exponentially to pre-fire levels two years after the fire

4. MODEL DEVELOPMENT

4.1. Overview

The results were used to develop a conceptual model of the processes driving increases in sediment exports following the fire. The very high measured values of I_{nc} indicate that broad scale *infiltration excess* overland flow is uncommon in this landscape, both prior to and after wildfire. Where overland flow does occur, both field data and the literature suggest that it is transient, and usually infiltrated a short distance down-slope into areas of high I_{nc} .

As a consequence of the conceptual model outlined above, in this catchment hillslope erosion processes are largely disconnected from the transport network (ie. the stream) due to the very high infiltration capacity of the forest soils. Only areas *immediately adjacent* to the stream contribute infiltration excess overland flow (and associated pollutants) to the stream edge under natural rainfall. Thus, near-stream and within-stream processes are central to the conceptual model, and most of the processes and properties

relevant to erosion prediction of *this* system lie within the riparian boundary.

An important component of this conceptual model is that the riparian fringe is able to generate infiltration excess overland flow even when the *infiltration capacity* of the soil exceeds the rainfall rate. This occurs because the high spatial variability in infiltration capacity results in some areas of low infiltration capacity being connected to the stream edge, even during low intensity rainfall events.

Saturation excess overland flow may also be generated in these near stream areas. However, measurements in other forests in steep landscapes suggest that these areas are probably only narrow in width due to the steep landscape and the high lateral hydraulic conductivity of the soils. Experiments are currently being developed to quantify the degree of saturation excess overland flow occurring in the East Kiewa catchments.

In summary, the total sediment load in these catchments is considered to be dominated by the following two processes;

1. sediment generated and transported from near-stream *infiltration excess* overland flow
2. sediment generated (re-mobilized) from within the stream channel due to decreased ET and increased peak flows (not considered further in this paper)

The remainder of this paper will focus on the development of an infiltration excess overland flow and erosion model, including the following elements;

- a function to represent runoff generation from areas with spatially variable I_{pc}
- a function to represent the seasonal oscillation in runoff generation due to water repellence, possibly as a function of the soil dryness index
- post-fire modification to this seasonal pattern as a function of time since the fire (not complete)
- a function to represent the change in interill sediment generation rates as a function of time since the fire

4.2. Runoff model for burnt forests

A spatially variable rainfall-runoff model was selected so that runoff was generated gradually, even when the rainfall rate was substantially less than the net infiltration capacity of the soil (ie. most of the time under natural rainfall conditions at this site). The model was modified to account for the effect of a seasonal oscillation in water repellence, and the effect of fire on this seasonal pattern.

The model is consistent with the theory presented by Hawkins and Cundy (1987) who showed that for an area with spatially variable infiltration there exist maximum and minimum curves relating the infiltration rate to the precipitation rate (Figure 3). The curves are derived by assuming an arrangement of point infiltration values that results in maximum or minimum infiltration rates, respectively. The true (but generally unknown) function relating precipitation rate to infiltration rate lies within these envelope curves. The key features of this model are that the infiltration rate is a function of *precipitation intensity* (rather than a function of *time* in traditional infiltration models), and that rainfall excess is generated even when the precipitation rate is lower than the net infiltration capacity of the plot.

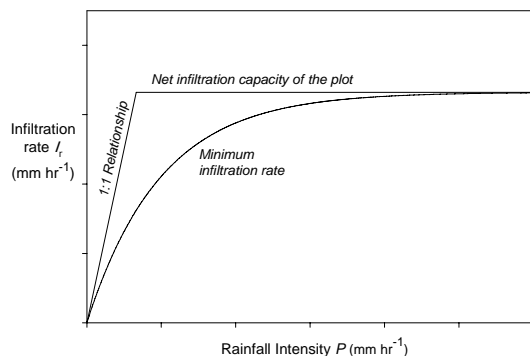


Figure 3. Hypothetical maximum and minimum envelope curves developed by Hawkins and Cundy (1987) for the relationship between precipitation and infiltration rate for an area with spatially variable infiltration capacity.

Following on from Hawkins and Cundy (1987) and Yu *et al.* (1997) the infiltration rate I_r is modeled as a function of the rainfall intensity P given by;

$$I_r = A(1 - \exp(-P/A)) \quad 1$$

The parameter A is determined implicitly by solving equation 1 using the mean of the measured steady-state infiltration rate from the three

replicates of the rainfall simulation experiments at each time-step. It should be noted that A is a fitting parameter and has no physical meaning unless it is assumed that the point values of infiltration are exponentially distributed and arranged from largest to smallest down the plot and that surface flow-paths are linear and parallel and steady state conditions have been reached. Under these conditions, the coefficient A can be interpreted as the net infiltration capacity I_{nc} of the plot, and equation 1 is equivalent to the minimum infiltration curve given in Figure 3. Yu *et al.* (1997; 1999) reported considerable success using equation 1 as the basis of a rainfall-runoff model.

A suitable expression relating the calculated values of A for *unburnt* treatments to the seasonal oscillation in soil dryness (and hence water repellence) can be given by;

$$A = \bar{A} - 2B \cos\left(\frac{2\pi d_i}{365.25}\right) \quad 2$$

Where d_i is the number of days since the peak of the drought index (Keech & Byram 1968), a broad-scale indicator of soil dryness. The drought index is calculated as a function of daily rainfall and maximum daily temperature. The coefficients \bar{A} and B were optimized by least squares regression to fit the experimental data shown in Figure 4, where the A values were calculated using equation 1 and measured I_r values from rainfall simulation.

Values for \bar{A} and B for the unburnt site were found to be 550 and 240 respectively. In Figure 4, the peak in the drought index is assumed to be the middle of summer (January 15). An improvement on equation 2 would be to use the value of the drought index itself as the independent variable, and this option is being explored further.

\bar{A} can be interpreted as the long-term mean value of A , and B is the amplitude of the seasonal oscillation in A . While in this case \bar{A} and B have been experimentally determined, it is expected that these parameters will eventually be able to be predicted as a function of soil properties, such as the susceptibility of the soil to water repellence.

Representation of the temporary inversion of this natural seasonal oscillation in runoff generation due to the fire (also shown in Figure 4) is not currently included in equation 2, and is the subject of ongoing work. One possibility is to make the amplitude B a function of time since the fire, allowing the function to tend towards the unburnt curve as time increases.

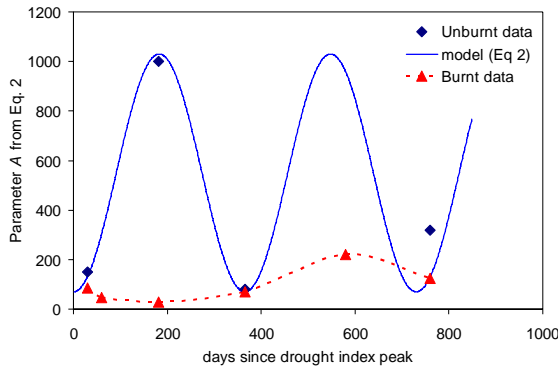


Figure 4. Temporal variation in the value of the infiltration equation parameter A from equation 1 for burnt and unburnt sites.

4.3. Interill sediment generation model

The interill sediment generation model is based on the idea that sediment generation from interill processes is approximately proportional to the square of the rainfall intensity. This was refined by Kinnell (1993) to the product of intensity and runoff rate, yielding the current Water Erosion Prediction Project (NSERL 1995) equation for the prediction of the interill erosion rate E_i ;

$$E_i = (QP)(K_i C_v) S_f \quad 3$$

Where Q is the plot discharge rate, P is the measured rainfall rate, K_i is an interill erodibility coefficient, C_v is an adjustment factor to account for reduced erosion due to vegetation cover, and S_f is an interill slope adjustment factor to account for the effect of slope on the interill erosion rate. Q is determined from;

$$Q = P - I_r \quad 4$$

Where the infiltration rate I_r is determined from equations 1 and 2. The WEPP (NSERL 1995) interill slope adjustment factor S_f in equation 3 is replaced by the logistic function S_i proposed by Sheridan *et al.* (2003);

$$S_i = \left(-1.5 + \frac{6.51}{1 + \exp(0.94 - 5.30 \sin \theta)} \right) \cdot \frac{1}{2.19} \quad 5$$

where θ is the slope angle and the factor of $1 / 2.19$ is an adjustment for use with the WEPP interill algorithm. Using this adjustment, both the WEPP interill slope adjustment factor (NSERL 1995) and equation 5 are equal at 9% slope. $(K_i C_v)$ are

considered together here and are determined as a function of days since the fire d_f from;

$$K_i C_v = (K_i C_v)_{ub} + G \exp(-d_f / 200) \quad 6$$

where $(K_i C_v)_{ub}$ is the interill erodibility and vegetation cover factor for the *unburnt* forest and G is given by;

$$G = (K_i C_v)_b - (K_i C_v)_{ub} \quad 7$$

$(K_i C_v)_b$ is the interill erodibility and vegetation cover factor for the *burnt* forest. Values of $(K_i C_v)_{ub}$ and $(K_i C_v)_b$ were determined by fitting equation 6 to the data shown in Figure 5, yielding 10,000 and 180,000 respectively.

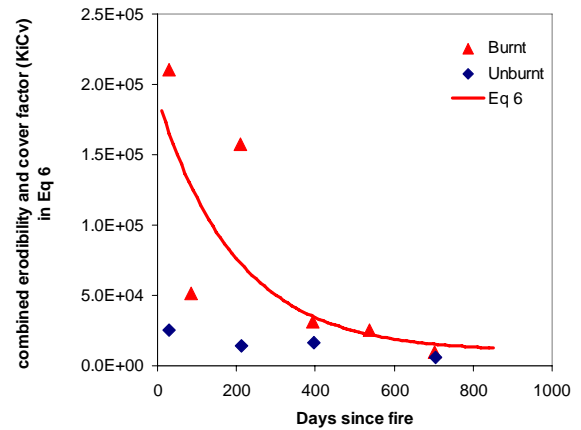


Figure 5. The relationship between the combined soil erodibility and vegetation factor and time since the fire (days).

Currently $(K_i C_v)$ are considered together by solving equation 3 using experimental data, however with further analysis these factors will be considered separately, both as a function of time since the fire. The vegetation cover adjustment factor C_v can be given as a function of the fractional (0-1) vegetation contact cover V by (NSERL 1995);

$$C_v = \exp(-2.5V) \quad 8$$

A suitable function for the change in vegetation cover V as a function of time since the fire has been developed from vegetation survey data shown in Figure 6.

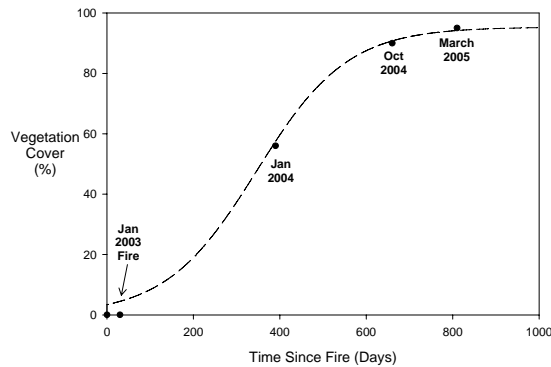


Figure 6. A sigmoidal function to represent the recovery of vegetation cover following the fire.

The recovery of surface contact cover following the fire is represented as a sigmoidal function of time since the fire, approaching an asymptote of 95% recovery in contact vegetation/litter cover in spring of 2004. The sigmoidal equation;

$$y = a + b / (1 + \exp(-(x - c) / d)) \quad 9$$

was fitted to the vegetation survey data yielding values for a , b , c , and d . A family of sigmoidal curves will be developed through selection of alternate constant values so as to represent slow, medium, and rapid rates of vegetation recovery.

5. CONCLUSIONS

The unexpected conclusion from this study is that the source of elevated post-fire stream sediment loads in these catchments is *not* broadscale hillslope erosion. Rather, the very high-spatially variable infiltration capacities result in infiltration excess overland flow and associated erosion from only a small hillslope fringe adjacent to the stream edge. Components of an erosion model are presented that aim to capture the dominant erosion processes observed in the post-fire catchment. Model development is continuing, and the model will be tested against measured sediment delivery rates at the catchment outlet.

6. ACKNOWLEDGMENTS

This project was funded under the Bushfire Recovery Program and the Parks and Forests research program, Department of Sustainability and Environment, Victoria, and from Land and Water Australia. Many thanks to Chris Sherwin for assistance with data analysis and graphics, and to Phil McKenna and Gabi Szegedy for laboratory and field assistance.

7. REFERENCES

- Hawkins, R.H., and Cundy, T.W. (1987), Steady-state analysis of infiltration and overland flow for spatially varied hillslopes. *Water Resources Bulletin* 23(2): 251-256.
- Keetch, J.J., and Byram, G.A. (1968), Drought index for forest fire control, Research Paper SE-38. U.S. Department of Agriculture, Forest Service, South-eastern Forest Experiment Station; 32.
- King, P.M. (1981), Comparison of methods for measuring the severity of water repellence of sandy soils and assessment of some factors that affect its measurement. *Australian Journal of Soil Research* 19: 275-285.
- Kinnell, P.I.A. (1993), Interill erodibilities based on the rainfall intensity-flow discharge erosivity factor. *Australian Journal of Soil Research* 31: 319-332.
- Lane, P., Sheridan, G.J., Noske, P., Costenaro, J., and Sherwin, C. (2004), The East Kiewa bushfire research catchments. Final Report to the Department of Sustainability and Environment, Victoria.
- NSERL (1995), USDA-Water Erosion Prediction Project (WEPP) Technical Documentation. National Soil Erosion Research Laboratory (NSERL) Report No 10. West Lafayette.
- Sheridan, G.J., Lane, P., Noske, P., and Sherwin, C. (2005), Quantification of the hillslope processes leading to elevated sediment and nutrient loads from burnt forested catchments. Unpublished Report for the Department of Sustainability and Environment, Victoria.
- Sheridan, G.J., Lane, P.N.J., Grayson, R.B., Noske P.J., Feikema, P. (2004), Preliminary analysis of pre- and post-bushfire water quality data from hydrologic stations in Eastern Victoria (Interim Report). Dept. of Sustainability and Environment.
- Sheridan, G.J., So, H.B., and Loch, R.J. (2003), Improved slope adjustment functions for soil erosion prediction. *Australian Journal of Soil Research*. 41(8): 1-20.
- Yu, B. (1999), A comparison of the Green-Ampt and a spatially variable infiltration model for natural storm events. *Trans ASAE*. 42(1): 89-97.
- Yu, B., Rose, C.W., Coughlan, K.J., and Fentie, B. (1997), Plot-scale rainfall-runoff characteristics and modelling at six sites in Australia and Southeast Asia. *Trans of the ASAE*. 40(5): 1295-1303.